

ELECTROMAGNETIC PROPERTIES OF LANTHANUM IRON GARNET FILLED PVDF-POLYMER COMPOSITE AT MICROWAVE FREQUENCIES USING FINITE ELEMENT METHOD (FEM) AND NICHOLSON-ROSS-WEIR (NRW) METHOD

HASSAN SOLEIMANI ^{a*}, NOORHANA YAHYA^a, MAZIYAR SABET^b, ZULKIFLY ABBAS^b, HOJJATOLLAH SOLEIMANI^b, GREGORY KOZLOWSKI^c, MOHAMMAD YEGANEH GHOTBI^d

^a*Fundamental and Applied Science Department, Universiti Teknologi PETRONAS, 31750 Seri Iskandar*

^b*Department of Physics, Faculty of Science, Universiti Putra Malaysia, 43400 UPM Serdang, Malaysia*

^c*Department of Physics, Wright State University, Dayton, OH, USA*

^d*Nanomaterials and Nanotechnology Program, Ceramics Engineering Department, Faculty of Engineering, University of Malayer, Malayer, Iran*

In our previous work, the lanthanum iron garnet-filled PVDF-polymer nanocomposite has been prepared. The real and imaginary parts of relative permittivity and permeability of mentioned sample were obtained simultaneously using the Nicholson-Ross-Weir (NRW) method based on the measurement of the reflection and transmission coefficients of the materials. In this study, the electric field distribution and attenuation at rectangular waveguide loaded sample were investigated based on the Finite Element Method (FEM). The computations of the reflection and transmission coefficients (S-parameters) were implemented using both the FEM and NRW methods. The results were compared with the measured reflection and transmission coefficients using the rectangular waveguide in conjunction with an Agilent N5230A PNA-L Vector network analyzer (VNA) at X-band frequencies (8 GHz- 12 GHz). The results of the relative error indicated that, among the two applied methods, the FEM is more accurate than the NRW method.

(Received June 16, 2013; Accepted December 21, 2013)

Keywords: Microwave measurements; RW-90 waveguide; LIG; PVDF; FEM; NRW

1. Introduction

The application of nanocomposites in microwave and electronic devices requires the exact knowledge of all parameters of a single wave carrier signal. Determination of reflection and transmission coefficients (S-Parameters) of garnet ferrites loaded polymer nanocomposites have attracted the interest of many researchers and scientists due to their applications in microwave and electronic devices such as isolators, filters and circulators [1-3].

As a soft ferrite material, lanthanum iron garnet ($\text{La}_3\text{Fe}_5\text{O}_{12}$) has been used in various applications in electronic devices. This is because of its efficient absorption of electromagnetic waves, low saturation flux density, low losses at high frequencies, high resistivity and easy to magnetize and demagnetize. As a result, polymer-based composites filled with ferrite particles, such as cobalt-ferrite [4], NiZn-ferrite [5], and MnZn-ferrite [6, 7] have attracted considerable attention over the years.

The parameters of a single wave carrier signal such as frequency, phase, and amplitude and DC component were determined by a general method based on four different samples [8]. The relative error of the estimated parameters was decreasing linearly as the signal-to-noise ratio

* Corresponding author: hassan.soleimani@petronas.com.my

(SNR) increases. For portable DSP, a simple and precise instantaneous frequency estimation method of single sinusoid signals were conducted based on instrumentation to obtain an analytical formula [9]. A quantized multiple sinusoids signal estimation algorithm was presented [10]. The accuracy of the initial values of iterations has a large influence on the speed of convergence. An iterative process was performed in order to reduce the cost function.

Many methods have been used for measuring reflection and transmission coefficients as electromagnetic properties of the materials [11,12]. In our previous work [13, 14], the transmission reflection rectangular waveguide technique (T/R) was conducted in order to obtain the reflection and transmission coefficients of the materials [15].

Moreover, in our previous studies, the Nicholson-Ross-Weir (NRW) method was applied to calculate simultaneously the complex permittivity and permeability of the lanthanum iron garnet-filled PVDF-polymer as nanocomposite sample [13]. The calculations were based on measured reflection and transmission coefficients of mentioned sample which positioned in rectangular waveguide at X-band frequencies. Inanition, The NRW method was introduced in order to calculate the reflection and transmission coefficients of the mentioned sample by applying obtained complex permittivity and permeability as well as [13, 15]. The comparisons of the results obtained by rectangular waveguide in conjunction with an Agilent N5230A PNA-L Vector network analyzer (VNA) and NRW method were presented to show the validation of obtained complex permittivity and permeability of sample [13].

Here, COMSOL software [16, 17] was used based on the Finite Element Method (FEM) to simulate the rectangular waveguide with three dimension of the geometry. The model consists of a rectangular waveguide with microwave propagation transition through it. This model applies the RF Module's Port boundary condition for the wave propagation problem. with this boundary condition, the software determines the distribution of the electric field intensity based on FEM [18], The attenuation of the PVDF-13%LIG was calculated in decibel (dB) based on the maximum intensity of electric field in rectangular waveguide where the wave enters and exits from it. The computations of the reflection and transmission coefficients were implemented using both the FEM and Nicholson-Ross-Weir (NRW) methods. The results were compared with the measured the reflection and transmission coefficient using the rectangular waveguide at X-band frequencies (8 GHz- 12 GHz). The Network analyzer was calibrated by implementing a standard full two-port calibration technique (SOLT).

2. Methodology

2.1 Finite Element Method

In this study, FEM was used in order to determine the reflection and transmission coefficients (S-Parameters) of PVDF-13%LIG which was loaded in rectangular waveguide as shown in Figure 1. It was assumed that the rectangular waveguide was excited by a dominant TE_{10} mode from the left and the reflection and transmission coefficient were measured at the reference plane s_1 and s_2 , respectively. For the purpose of analysis, the rectangular waveguide are divided into three regions: Region I ($z < 0$) and Region II ($0 \leq z \leq d$) and Region III ($z > 0$). While the first and third regions (I and III) were covered by air the nanocomposite sample located in the second region (II).



Fig. 1. Rectangular Waveguide Loaded with PVDF-13%LIG Sample

In the FEM formulation, the electric field in the rectangular waveguide was discretized using tetrahedron elements [19, 20]. Hence, within each tetrahedron, the unknown field can be interpolated from each node value by using the first order polynomial [21] as follows:

$$\rho^e(x, y, z) = a^e + b^e x + c^e y + d^e z \quad (1)$$

The electric field in the rectangular waveguide is

$$\mathbf{E}^e = \sum_{i=1}^6 N_i^e \mathbf{E}_i^e(x, y, z) \quad (2)$$

where N_i^e , $i = 1, 2, 3 \dots 6$ are the six complex amplitudes of electric field associated with the six edges of the tetrahedron, and $\mathbf{E}_i^e(x, y, z)$ is the vector basis function associated with the i^{th} edge of the tetrahedron. Substituting equation (1) with equation (2) and using the boundary condition and the integration over the volume of one Tetrahedron is now:

$$\begin{aligned} \frac{1}{\mu_r} \cdot (\sum_{i=1}^6 N_i^e \iiint (\nabla \times \vec{W}_j \cdot \nabla \times \vec{W}_i - k_0^2 \epsilon_r \vec{W}_i \cdot \vec{W}_j) dv = 2 \left(\frac{j\omega\mu}{\mu_r} \right) \cdot Y_0^l \cdot \iint \vec{W}_j \cdot \vec{e}_0(x, y) ds \\ - \left(\frac{j\omega\mu}{\mu_r} \right) \sum_{i=1}^6 N_i^e \sum_{p=0}^{\infty} Y_p^l (\iint \vec{W}_j \cdot \vec{e}_p(x, y) ds \cdot \iint \vec{W}_i \cdot \vec{e}_p(x, y) ds) \end{aligned} \quad (3)$$

After the simplification, the matrix form of equation (3) can be written as follows:

$$\begin{pmatrix} S_{11}^e & \dots & S_{16}^e \\ \vdots & \ddots & \vdots \\ S_{61}^e & \dots & S_{66}^e \end{pmatrix} \begin{pmatrix} N_1^e \\ \vdots \\ N_6^e \end{pmatrix} = \begin{pmatrix} V_1^e \\ \vdots \\ V_6^e \end{pmatrix} \quad (4)$$

where the elements of matrices are given by:

$$\begin{aligned} S_{el}(j, i) = \frac{1}{\mu_r} \iiint (\nabla \times \vec{W}_j \times \nabla \times \vec{W}_i - k_0^2 \epsilon_r \vec{W}_i \times \vec{W}_j) dv \\ + \left(\frac{j\omega\mu}{\mu_r} \right) \sum_{p=0}^{\infty} Y_p^l (\iint \vec{W}_j \times \vec{e}_p(x, y) ds \times \iint \vec{W}_i \times \vec{e}_p(x, y) ds) \end{aligned} \quad (5)$$

$$v(j) = 2 \left(\frac{j\omega\mu}{\mu_r} \right) \times Y_0^l \times \iint \vec{W}_j \times \vec{e}_0(x, y) ds \quad (6)$$

These element matrices can be assembled over all the tetrahedron elements in the sample region to obtain a global matrix equation

$$[S] \times \{N_i\} = \{v\} \quad (7)$$

The solution vector $\{N_i\}$ of matrix equation (7) is then used to determine the reflection and transmission coefficients at the reference plane S_1 and S_2 [22].

$$R = \iint \vec{E}|_{\text{over } S_1} \times \vec{e}_0 ds - 1 \quad (8)$$

$$T = \iint \vec{E}|_{\text{over } S_2} \times \vec{e}_0 ds \quad (9)$$

The reflection and transmission coefficient of the wave defined in above (equations 8 and 9) are used in the COMSOL software.

2.2 Sample Preparation

LIG was prepared according to the previous our work [23]. Amorphous LIG was synthesized by sol-gel method. The pure phase crystalline cubic LIG was obtained by the heat-treatment of the as-prepared amorphous material at 700 °C for 2h in air atmosphere. PVDF-

13%LIG as a nanocomposite sample was prepared by solvent method with 13 % filler and 87 % of PVDF in the form of a rectangular sheet with 3 mm thickness.

2.3 Experimental Method

PVDF-13%LIG as nanocomposite sample was snugly fitted into a WR-90 waveguide then reflection and transmission coefficients were measured in the frequency range of 8 -12 GHz by using an Agilent N5230A PNA-L network analyzer. In this technique the fundamental transverse electromagnetic (TEM) mode is the only mode that propagates in rectangular waveguide. Network analyzer was calibrated by implementing a standard full two-port calibration technique (SOLT) for 201 frequency points. The experiments carried out at room temperature.

3. Results and discussion

3.1 Material characterization

Characterization of the sample has been carried out by various techniques as the results have been reported in our previous work [23].

3.2 Complex Permittivity and Permeability

In our previous study, The NRW method was applied to determine simultaneously the real and imaginary parts of complex permittivity and permeability of PVDF-13%LIG based on measured reflection and transmission coefficients. The results indicated that the decreasing in real and imaginary part of complex permeability and real part of complex permittivity resulted in increasing the frequency; meanwhile imaginary part of permittivity tends to become constant when frequency increased. The mean values of real and imaginary parts of the complex permittivity and permeability of mentioned sample at X-band frequencies were $(4.33-j0.09)$ and $(1.24-j0.15)$ respectively [13].

3.3 Electric field distribution

In order to simulate rectangular waveguide loaded mentioned nanocomposite sample FEM was applied. Figure 2 show the 2D plot of FEM simulated rectangular waveguide loaded sample. General observation shows that the essential differences of emitted electric field intensity in difference regions of rectangular waveguide at 12 GHz.

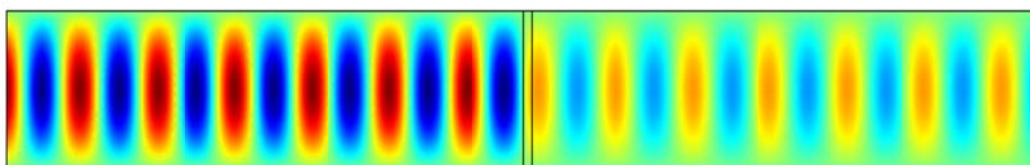


Fig. 2. FEM Simulation of Electric Intensity for 3 mm thick of PVDF-13%YIG in 2D Surface Plots

Figure 3(a, b, c) Show the variation of z component of the electrical field versus the length of the rectangular waveguide. The X axis represents the length of a rectangular waveguide from - 0.2 to 0.2 m, and the z axis indicates the z component of the electric field.

In region (I) of waveguide which loaded the air, the maximum electric field amplitude presented was as high as 385 V/m that is shown in Figure 3 (a). When the wave was propagated through the sample, the electric field amplitude decreased to 144 V/m. As can be seen in Figure 3(b), only 0.275 % of one wavelength of propagated wave appears in region II due to 3 mm thickness of sample and 2.30 as value of the refractive index of PVDF-13% LIG [13] which confirms the validation of FEM simulation results. This result as percentage of one wavelength of propagated wave at 3 mm thickness of PVDF-13% LIG is expected where the wavelength of propagated wave in mentioned sample at 12 GHz frequency has a value of 10.86 mm. The Figure 3(c) shows that the electrical field amplitude increased to 146 V/m where the wave exiting from

the region II to the region III of rectangular waveguide. Therefore, the attenuation of a 3 mm thick of mentioned sample at 12 GHz frequency was achieved at 9.30 dB which it was due to the maximum intensity of electric fields in entrance region I and exit from region III at rectangular waveguide.

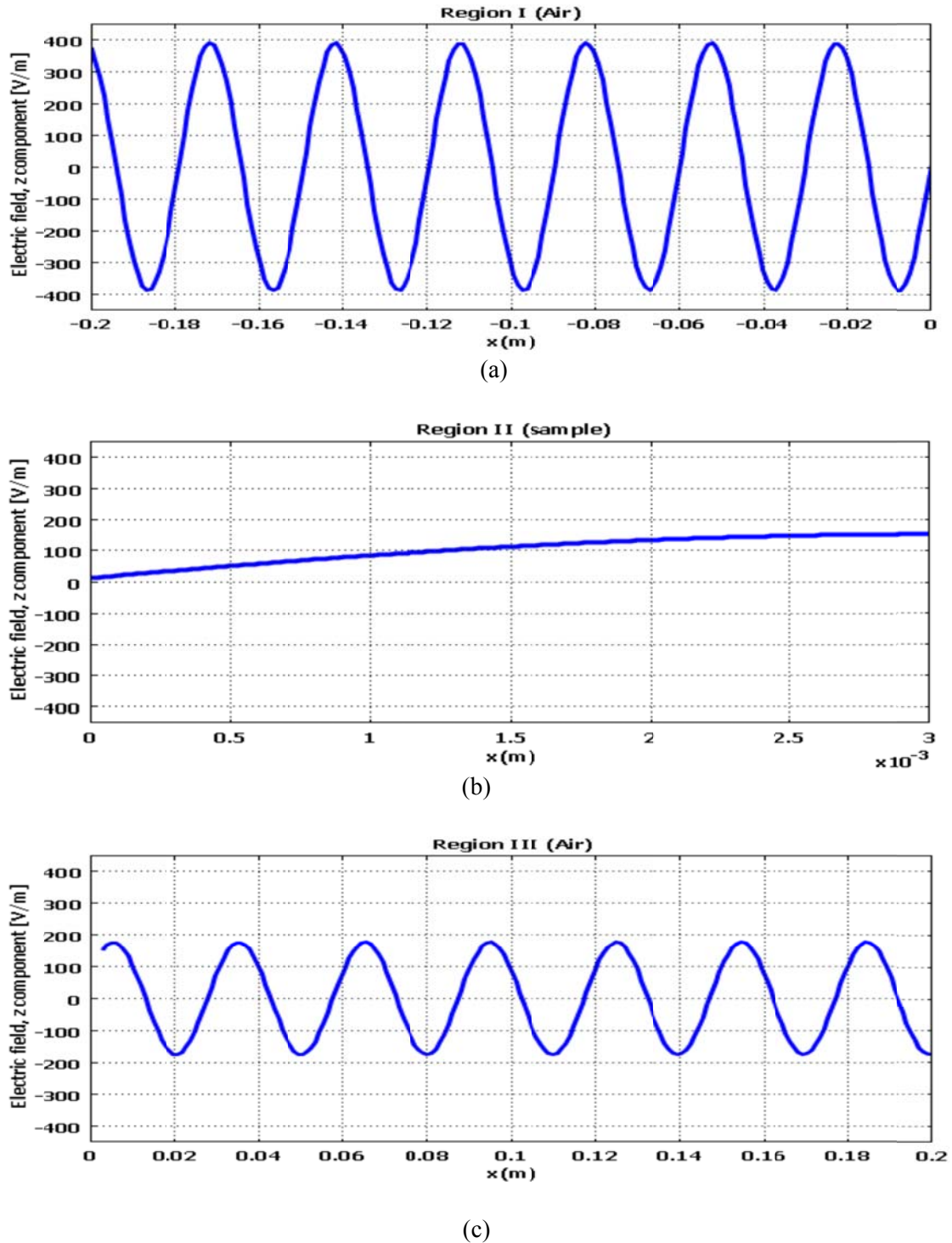


Fig. 3: Variation of the z Component of Electric Field with respect to the Length of Rectangular Waveguide in (a) Region I, (b) Region II, and (c) Region III

3.4 Reflection and Transmission Coefficient

Fig. 4(a, b) shows the comparisons between the FEM simulation, NRW Method results and measured data for variation in the reflection and transmission coefficients of PVDF-13%LIG with frequency where placed in the rectangular waveguide. As shown in mentioned Figure, the X-axis represents the frequencies from 8 to 12 GHz and the Y-axis indicates a tolerance from zero to one. General observation indicates that the level of transmission is greater than reflection. The sum of reflection and transmission coefficients values is always around unity. Hence, the increase in reflection coefficient causes the decrease of transmission coefficient and vice versa.

As can be seen in mentioned figure, the measured, calculated (NRW) and simulated (FEM) values for reflection coefficients start at 0.54, 0.38 and 0.64 respectively from the Y axis. From this point, the trend of the measured and simulated curves of reflection coefficient demonstrates a decreasing to 0.52 and 0.53 when the frequency reaches to the 12 GHz, Meanwhile, the calculated curve of reflection coefficient demonstrates an increasing trend up to 0.42 when the frequency reaches 12 GHz. In contrast, from the Y axis, the measured, calculated (NRW) and simulated (FEM) values in transmission coefficient start at 0.70, 0.87 and 0.64 respectively. From this point, the trend of the measured and simulated curves almost remains constant to the final frequency of 12 GHz. Meanwhile, the calculated curve of transmission coefficient demonstrates a decrease to 0.76 when the frequency reaches 12 GHz in the X axis.

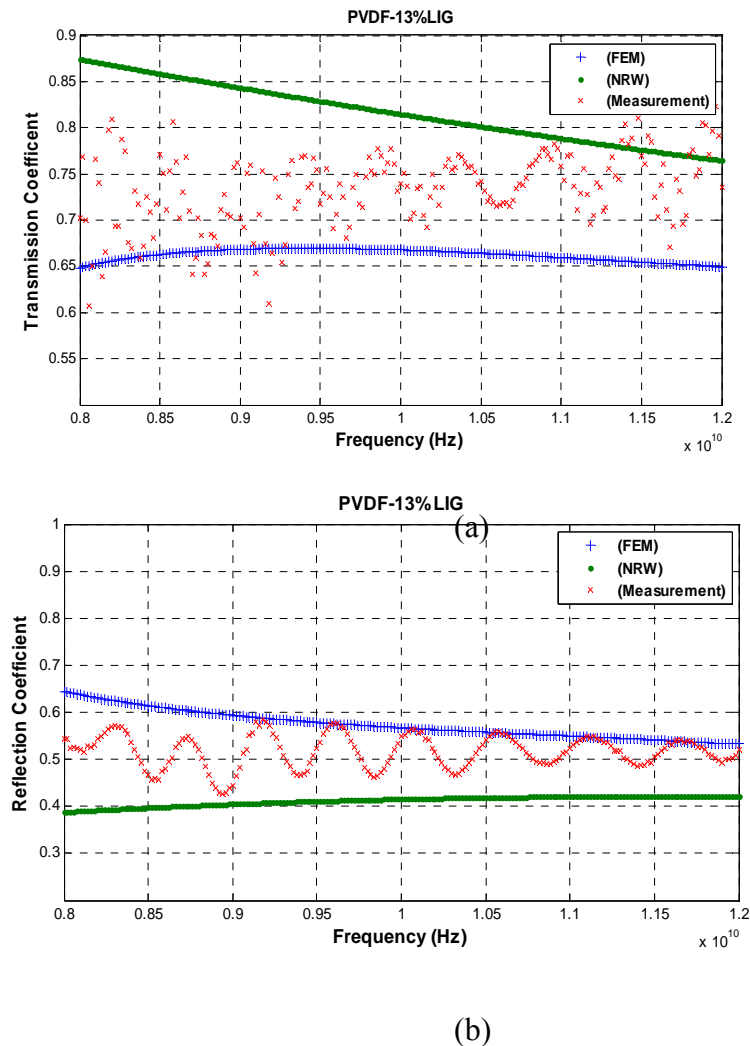


Fig. 4. Measured, calculated and simulated magnitude of a) transmission and (b) reflection coefficient of a 3 mm thick of PVDF-13%LIG at X-band Frequencies

The accuracy of FEM simulation and calculated (NRW) of reflection and transmission coefficients can be determined by calculating the relative error with respect to the measurement data. The mean relative error values of FEM simulation of reflection and transmission coefficients observed to 0.0596 and 0.0972, respectively meanwhile The mean relative error values of calculated (NRW) of the reflection and transmission coefficients observed to be 0.2417 and 0.1110, respectively. Consequently, the results indicate that the obtained results by FEM method are more accurate than NRW method where PVDF-13%LIG is examined. Hence, The FEM is highly suggested in order to obtain electromagnetic properties of nanocomposites.

4. Conclusions

In this work, the Finite Element Method (FEM) procedure has been presented to determine the distribution of electric field intensity of the 3 mm thick of PVDF-13%LIG as nanocomposite sample which was placed in rectangular waveguide. The results indicated that the attenuation of mentioned nanocomposite sample at 12 GHz frequency revealed to 9.30 dB. Furthermore, the magnitudes of the reflection and transmission coefficients of the PVDF-13%LIG were obtained successfully by FEM, NRW and experimental method as well. General observations on curves indicate that the level of transmission is greater than reflection. In addition, it can be deduced that the reflection and transmission coefficients obtained by FEM are more accurate than achievements results by NRW method due to the values of mean relative error.

Acknowledgments

The authors would like to acknowledge Universiti Teknologi PETRONAS (UTP) for all the facilities and research support by providing the YUTP Grant and Institute of Advanced Technology of Universiti Putra Malaysia (UPM) for its facilities and laboratory.

References

- [1] P. Toneguzzo, O. Acher, G. Viau, F. Fievet-Vincent, F. Fievet, *J. Appl. Phys.* **81**(8), 5546 (1997).
- [2] Pardavi-Horvath, M., *J. Magn. Magn. Mater.* **203**(1-3), 57-59 (1999),
- [3] Wu, Y.J.; Fu, H.P.; Hong, R.Y.; Zheng, Y.; Wei, D.G. *J. Alloys Compd.*, **470**, 497 (2009).
- [4] Vaishnava, P.P.; Senaratne, U.; Buc, E.; Naik, R.; Naik, V.M.; Tsoi, G.; Wenger, L.E.; Boolchand, P. *J. Appl. Phys.*, **99**(8), 08G702 (2006).
- [5] Nakamura, T; Tsutaoka, T.; Hatakeyama, K. *J. Magn. Magn. Mater.*, **138**, 319-328 (1994)
- [6] Yavuz, O.; Ram, M.K.; Aldissi, M.; Poddar, P.; Hariharan, S. *J. Mater. Chem.*, **15**, 810 (2005)
- [7] Kazantseva, N.E.; Bespyatykh, Y.I.; Sapurina I.; Stejskal J.; Vilcáková J.; Sába, P. *J. Magn. Magn. Mater.*, **301**, 155 (2006)
- [8] Vizireanu, D.N; Halunga, S.V. *International Journal of Electronics*, **98**(7), 941 (2011)
- [9] Vizireanu, D.N. *Journal of Measurement*, **44**(2), 500 (2011).
- [10] Udrea, R.M.; Vizireanu, D.N. Quantized multiple sinusoids signal estimation algorithm. *J. of Instrumentation (JINST)* **3**, 1 (2008).
- [11] Baker-Jarvis, J. Dielectric and magnetic measurement methods in transmission lines: An overview. *Proceedings of the 1992 AMTA Workshop, Chicago, Illinois. 1992.*
- [12] Simsek, S; Isik, C.; Topuz, B. *Esen, AEU-International Journal of Electronics and Communication*, **60**(9), 677 (2006).
- [13] Soleimani, H.; Abbas, Z.; Yahya, N.; Soleimani, H.; Ghotbi, M.Y., *Measurement* **45**, 1621 (2012).
- [14] Soleimani, H.; Abbas, Z.; Yahya, N.; Shameli, K.; Soleimani, H.; Shabanzadeh, P. *International Journal of Molecular Sciences.*, **13**(7), 8540 (2012).
- [15] Lighthart, L.P. *IEEE Trans. Microw. Theo. Tech.* **31**, 249 (1983)

- [16] Soleimani, H.; Abbas, Z.; Khalid, K; Yahya, N; Soleimani, H. *European Journal of Scientific Research*, **39**(1), 105 (2010)
- [17] COMSOL Multiphysics Model Library, ver. 3.3; Comsol AB, 2006.
- [18] Sadiku, M. N. O. *Elements of electromagnetic*; Oxford University Press: New York, 2001.
- [19] Silvester, P. P.; Ferrari, R. L. *Finite Elements for Electrical Engineers*, 2nd ed.; Cambridge Univ. Press: 1990.
- [20] Reddy, C. J.; Deshpande. M. D.; Cockrell, C.R.; Beck F.B. *Finite element method for eigenvalue problems in electromagnetic*. NASA Technical Paper 3485, 1994.
- [21] Reddy, C. J., Deshpande, M. D. *Application of FEM to estimate complex permittivity of dielectric material at microwave frequency using waveguide measurements*. NASA Contractor Report, 1995.
- [22] Coccioli, R.; Pelosi, G.; Selleri, S. *Characterization of Dielectric Materials with the Finite-Element Method*. *IEEE Transactions on Microwave Theory and Techniques*, 4(77) (1999).
- [23] Soleimani, H.; Abbas, Z.; Yahya, N; Soleimani, H.; Ghotbi, M.Y. *Journal of Composite Materials*, **46**(12), 1497 (2012)